Available online at www.sciencedirect.com
SCIENCE DIRECT®
Fluid Dynamics Research 38 (2006) 405–429
FLUID DYNAMICS RESEARCH

Effect of viscous dissipation on the Darcy free convection boundary-layer flow over a vertical plate with exponential temperature distribution in a porous medium

E. Magyari[a,*], D.A.S. Rees[b]

[a] *Chair of Physics of Buildings, Institute of Building Technology, Swiss Federal Institute of Technology (ETH) Zürich, Wolfgang-Pauli-Str.1, CH-8093 Zürich, Switzerland*
[b] *Department of Mechanical Engineering, University of Bath, Claverton Down, Bath, BA2 7AY, UK*

Accepted 8 February 2006

Communicated by M. Oberlack

Abstract

The title problem is investigated for an upward projecting hot plate ("upflow") and for its downward projecting cold counterpart ("downflow"). When viscous dissipation is negligible, these two cases are physically equivalent, but the heat released by viscous friction breaks the equivalence between the upflow and downflow cases, and substantial differences occur. In particular, we find that, for self-similar flows, downflow is possible for all nonnegative values of the temperature exponent, but upflow only exists above a critical value of this parameter, which equals the half of the Gebhart number of the fluid. Each two upflow and downflow solution branches were found, respectively. All the corresponding solutions decay exponentially with increasing distance from the plate. It could be shown that these up and downflow solution branches do not represent in fact two isolated solutions but, they are the limiting cases of respective families of intermediate solutions which are bounded between the branches, and which decay algebraically in the transversal far field. This paper investigates in detail the heat transfer characteristics of all these self-similar free convection flows analytically and numerically.

Keywords: Free convection; Viscous dissipation; Boundary layer; Exponential similarity; Critical exponent

* Corresponding author.
E-mail address: magyari@hbt.arch.ethz.ch (E. Magyari).

0169-5983/$30.00 © 2006 The Japan Society of Fluid Mechanics and Elsevier B.V. All rights reserved.
doi:10.1016/j.fluiddyn.2006.02.005

1. Introduction

Since the early paper of Goldstein (1939) it has been known that the boundary layer equations for clear fluids allow for two basic types of self-similar solution as a requirement of their scaling invariance. These are the power-law and of exponential types, respectively. These statements also hold for free convection flows over vertical plates for both clear viscous fluids and saturated porous media, but only when the effect of viscous dissipation is neglected. When the viscous dissipation term is included in the energy equation, self-similarity cannot exist for the power-law cases. Therefore, the exponential type forms are the only possible case for self-similarity, as was first pointed out by Gebhart and Mollendorf (1969) for the free convection of clear fluids and by Nakayama and Pop (1989) for the free convection in saturated porous media. This circumstance suggests that concerning the self-similarity the exponential laws posses a certain universality. It is worth mentioning in this respect that the exponential mean velocity profile also allows for the self-similarity of the velocity correlation equations arising in the statistical theory of turbulent flows, as being discovered recently by Oberlack (2000, 2001, 2004).

The present paper is concerned with the effect of viscous dissipation on self-similar Darcy free convection flow over an impermeable semi-infinite vertical plate adjacent to a saturated porous medium where the heated surface has an exponential temperature distribution of the form

$$T_w(x) = T_\infty + sT_0 \exp\left(a\frac{x}{L}\right). \tag{1}$$

Here x is the wall coordinate measured from the definite edge of the plate and L a reference length. The logarithmic increment a of the wall temperature distribution is assumed to be nonnegative. The special case $a = 0$ corresponds to the well-known but important particular case of the isothermal plate. T_∞ is the ambient temperature, and T_0 the positive constant given by $T_0 = |T_w(0) - T_\infty|$. In addition, $s = +1$ for a hot plate ($T_w > T_\infty$, "upflow") and $s = -1$ for a cold plate ($T_w < T_\infty$, "downflow"), respectively.

A remarkable qualitative effect of viscous dissipation is that its presence breaks the physical equivalence between the free convection upflow due to an upward projecting hot plate on the one hand, and the free convection downflow due to a downward projecting cold plate on the other hand. Some consequences of this phenomenon were investigated recently by Magyari and Keller (2003) and Rees et al. (2003) for isothermal plates adjacent to a saturated porous medium. The main focus of the present paper is to examine the detailed mechanical and thermal characteristics of the up- and downflow cases for the wall temperature distribution (1) by means of analytical and numerical methods.

2. Basic equations

Following Nield and Bejan (1999) we write the continuity, Darcy and energy equations for free convection flow over a semi-infinite vertical flat plate adjacent to a saturated porous medium in the form

$$u_x + v_y = 0, \tag{2}$$

$$u_y = s_g \frac{g\beta_T K}{\upsilon} T_y, \tag{3}$$

$$uT_x + vT_y = \alpha T_{yy} + \frac{\upsilon}{Kc_p} u^2, \tag{4}$$

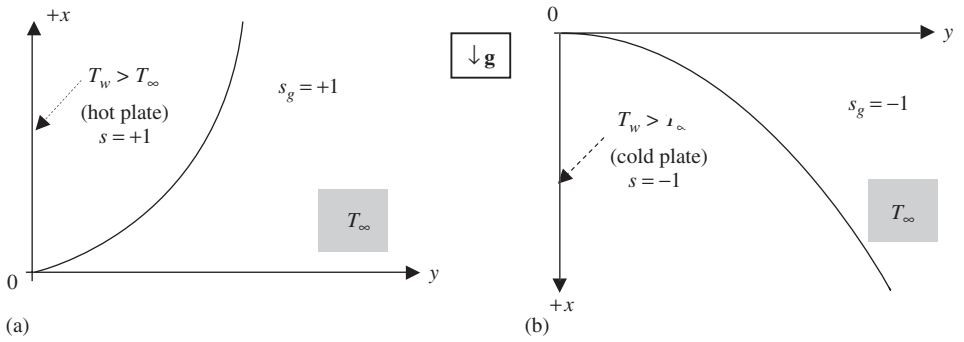

Fig. 1. (a,b). Coordinate system for the up- and downflow domains. As a consequence of the heat released by viscous dissipation, the two situations (a) and (b) become physically distinct. Some typical velocity and temperature profiles are shown in Figs. 3, 7 and 8.

where we have assumed that the boundary-layer and the Boussinesq approximations hold. The second term on the right-hand side of Eq. (4) is proportional to the volumetric heat generation rate by viscous friction $q''' \equiv \mu u^2/K$.

In the above equations $x \geqslant 0$ and $y \geqslant 0$ are the Cartesian coordinates along and normal to the plate, respectively, u and v are the velocity components along x and y axes, T is the fluid temperature, K the permeability of the porous medium, g the acceleration due to gravity, $s_g = +1$ or -1 when the x-axis is directed vertically upwards or downwards, respectively (see Figs. 1a,b), c_p is the specific heat at constant pressure, α, β_T and $\upsilon = \mu/\rho$ are the effective thermal diffusivity, thermal expansion coefficient and kinematic viscosity, respectively, and the subscripts x and y indicate partial derivatives. This choice of the coordinate system implies that $s_g = s = \pm 1$ (see Figs. 1a,b). The plate is considered to be impermeable. Thus, the boundary conditions are:

$$\begin{aligned} &v = 0, \quad T = T_w(x) \quad \text{on } y = 0, \\ &u \to 0, \quad T \to T_\infty \quad \text{as } y \to \infty, \end{aligned} \tag{5}$$

where $T_w(x)$ is given by Eq. (1).

Specifying the wall temperature at the leading edge $T_w(0)$, and at some distance $x = L$ from it, $T_w(L)$, its logarithmic increment a is given uniquely by

$$a = \ln \left| \frac{T_w(L) - T_\infty}{T_w(0) - T_\infty} \right|. \tag{6}$$

Eq. (3) can be integrated immediately. Bearing in mind the boundary condition (5), we obtain

$$T = T_\infty + s \frac{\upsilon}{g\beta_T K} u. \tag{7}$$

Furthermore, on introducing the dimensionless coordinates $X = x/L$, $Y = y/L$ and velocity components $U = (L/\alpha)u$, $V = (L/\alpha)v$ and substituting Eq. (7) in Eq. (4), we obtain the dimensionless velocity equation,

$$UU_X + VU_Y = U_{YY} + sGeU^2 \tag{8}$$

where Ge denotes the Gebhart number, $Ge = g\beta_T L/c_p$. We see that the Gebhart number specifies the "weight" of the viscous dissipation in the energy balance.

Due to the presence of the sign $s = \pm 1$ in Eq. (8), an important qualitative effect of viscous dissipation becomes manifest. It shows that the well-known textbook result, according to which the free convection flows over an upward projecting hot plate ($s = +1$, Fig. 1a) and over its downward projecting cold counterpart ($s = -1$, Fig. 1b) are physically equivalent, holds only when viscous dissipation is neglected ($Ge = 0$) in the energy equation. If, however, viscous dissipation is taken into account ($Ge \neq 0$), this physical equivalence is broken and the "upflow" (Fig. 1a) and the "downflow" (Fig. 1b) situations become physically distinct. As has been reported recently by Magyari and Keller (2003) and Rees et al. (2003), one of the important consequences of this broken equivalence is the existence of a strictly parallel free convection flow, the so-called asymptotic viscous dissipation profile (ADP), which can only occur over a downward projecting isothermal cold plate (the particular case $a = 0$, $s = -1$ of the present problem, see Section 5.6), but not over its upward projecting hot counterpart. Substantial differences also occur between the upflow and downflow cases for the nonisothermal plate ($a \neq 0$), and these will be discussed in detail in Sections 4–7.

It is worth underlining here that the broken upflow/downflow equivalence as an effect of viscous dissipation is in full agreement with the first principle of thermodynamics since it is a direct consequence of the energy balance equation. A basic difference between the free convection up- and downflows in the presence of viscous friction (leading to broken equivalence mentioned) consists of their different *thermodynamic efficiency*, i.e. of the useful work ("exergy") generated in these processes as a consequence of the second law of thermodynamics. Indeed, the natural convection past a heated vertical plate can be regarded as an infinite sequence of convection loops, one nested inside the next, each of them consisting of a *heating* $\rightarrow$ *expansion* $\rightarrow$ *cooling* $\rightarrow$ *compression* sequence, similarly to the cycles executed by the working fluid in a heat engine (see Bejan, 1995, Fig. 4.1, p. 157). Hence, inserting in these convection loops a suitably designed propeller we can gain useful mechanical work. In absence of viscous dissipation, "Bejan's free convection heat engine" works reversibly. Its cycles produce the same useful work both from an upward projecting hot plate and from its downward projecting cold counterpart. However, the volumetric heat generation by viscous dissipation is associated according to the second law of thermodynamics with an entropy production and thus with a partial or even total destruction of exergy delivered by the irreversible cycles of the free convection heat engine (Bejan et al., 2004). While in the *fluid cooling* situation of the cold isothermal plate the heat released by viscous friction enhances the (negative) wall heat flux and thus it is removed from the fluid, in the *fluid heating* situation of the isothermal hot plate it diminishes the (positive) heat flux from the wall to the fluid and thus also the useful work delivered. In the limiting case of the *parallel* free convection flows, the entropy production and exergy destruction during the transient flow regime over the hot plate can even reach their extreme values, such that in the steady regime the delivery useful work from the hot plate shrinks to zero.

3. Similarity transformation

In terms of the dimensionless stream function ψ defined by equations

$$u = \frac{\alpha}{L}\psi_Y, \quad v = -\frac{\alpha}{L}\psi_X \tag{9}$$

the continuity equation (2) is satisfied identically and Eqs. (7) and (8) become

$$T = T_\infty + s\frac{T_0}{Ra}\,\psi_Y, \tag{10}$$

$$\psi_Y\psi_{XY} - \psi_X\psi_{YY} = \psi_{YYY} + sGe\psi_Y^2, \tag{11}$$

where $Ra = g\beta_T KLT_0/(\upsilon\alpha)$ denotes the Darcy–Rayleigh number.

In order to obtain the governing self-similar equations corresponding to the wall temperature distribution (1), we introduce the transformations

$$\psi = (Ra/Ge)^{1/2}\mathrm{e}^{a/2X} f(\eta), \quad \eta = (GeRa)^{1/2}\mathrm{e}^{a/2X} Y. \tag{12}$$

In this way the similarity solution of the problem (1)–(5) is obtained as follows:

$$u = \frac{\alpha}{L}\,Ra\mathrm{e}^{aX} f'(\eta), \tag{13}$$

$$v = -\frac{\alpha}{L}\,\frac{a}{2}\left(\frac{Ra}{Ge}\right)^{1/2}\mathrm{e}^{a/2X}[f(\eta) + \eta f'(\eta)], \tag{14}$$

$$T = T_\infty + sT_0\mathrm{e}^{aX} f'(\eta). \tag{15}$$

Here the similar stream function f satisfies the ordinary differential equation

$$f''' + \frac{\gamma}{2}\,ff'' + (s-\gamma)f'^2 = 0 \tag{16}$$

along with the boundary conditions

$$f(0) = 0, \quad f'(0) = 1, \quad f'(\infty) = 0, \tag{17}$$

where the primes denote derivatives with respect to η and

$$\gamma = \frac{a}{Ge}. \tag{18}$$

The velocity and temperature fields (13)–(15) are fully determined if the dimensionless stream function $f = f(\eta)$ is known. In particular, $f'(\eta)$ corresponds to both the streamwise velocity component, u, as well as the temperature field, T. Therefore, the basic task is to solve the two-point boundary value problem (16), (17). The presence of the sign, s, in Eq. (16) recalls again the essential difference between the up- and downflow if the viscous dissipation is taken into account ($Ge \neq 0$).

The quantity of the main engineering interest is the wall heat flux

$$q_w(x) = -k\left.\frac{\partial T}{\partial y}\right|_{y=0} = -s\frac{k}{L}\left(\frac{aRa}{\gamma}\right)^{1/2} T_0\mathrm{e}^{3/2aX} f''(0), \tag{19}$$

where k denotes the effective thermal conductivity of the fluid saturated porous medium. Thus, the wall temperature gradient function, $f''(0)$, is a quantity of basic interest in the present investigation. Eq. (16)

and the boundary conditions (17) yield the following integral relationship for $f''(0)$:

$$f''(0) = \left(s - \frac{3\gamma}{2}\right) \int_0^\infty f'^2(\eta)\, \mathrm{d}\eta. \tag{20}$$

This relationship holds for all the solutions which satisfy the condition,

$$\lim_{\eta\to\infty} f(\eta) f'(\eta) = 0. \tag{21}$$

Eq. (20) implies that

$$f''(0) = 0 \quad \text{for} \quad \gamma = \frac{2}{3} s \tag{22a}$$

and

$$\mathrm{sgn}[f''(0)] = \mathrm{sgn}\left(\frac{2}{3} s - \gamma\right) \text{for} \quad \gamma \neq \frac{2}{3} s. \tag{22b}$$

Therefore,

$$\mathrm{sgn}[q_w(x)] = \mathrm{sgn}[-s f''(0)] = \mathrm{sgn}\left(s\gamma - \frac{2}{3}\right) \tag{23}$$

and thus $q_w > 0$ (direct wall heat flux; plate heats the fluid) for $s\gamma > \frac{2}{3}$ and $q_w < 0$ (reversed wall heat flux; fluid heats the plate) for $s\gamma < \frac{2}{3}$, respectively.

4. General features of the solutions

In the subsequent discussion of solutions it will be convenient to introduce, in addition to the parameter $\gamma = a/Ge$, an alternative parameter, m, defined by

$$\gamma = s(1 + m). \tag{24}$$

Thus, Eq. (16) becomes

$$f''' + s\left[\frac{m+1}{2} f f'' - m f'^2\right] = 0. \tag{25}$$

The condition $a > 0$ requires that

$$\begin{aligned} &m > -1 \quad \text{for upflows } (s = +1), \\ &m < -1 \quad \text{for downflows } (s = -1). \end{aligned} \tag{26}$$

For the isothermal plate ($a = 0$) only a downflow solution exists which is precisely the ADP (see Sections 4.2 and 5.6).

4.1. Upflows

For the case of upflows ($s = +1$) Eq. (25) reduces to the one first obtained by Cheng and Minkowycz (1977) for the title problem of the present paper but on assuming that

(i) the plate temperature distribution is of the power-law form, $T_w(x) = T_\infty + T_0 X^m$,
(ii) the effect of viscous dissipation may be neglected.

The connection between the present exponentially similar problem and the Cheng–Minkowycz power-law similarity equation has already been noted by Nakayama and Pop (1989).

Cheng and Minkowycz (1977) solved Eq. (25) numerically for $s = +1$ along with the boundary conditions (17) with the power-law exponent in the range $-\frac{1}{3} < m < 1$. A comprehensive study was then performed by Ingham and Brown (1986) who proved rigorously that the Cheng–Minkowycz problem does not admit solutions in the parameter range $m \leqslant -\frac{1}{2}$. Later, several analytical and numerical solutions of this problem were collected in the monograph of Pop and Ingham (2001). The following features of the *upflow* solutions of the present problem may be extracted from the many studies of the Cheng–Minkowycz problem:

1. Upflow solutions only exist above the critical value $\gamma_{\text{crit}} = \frac{1}{2}$ of the parameter γ, i.e. above the value $a_{\text{crit}} = Ge/2$ of the temperature exponent a. This follows from Eq. (24) and the result of Ingham and Brown (1986) mentioned above.
2. In the range $\gamma_{\text{crit}} < \gamma < 1$ (i.e. $-\frac{1}{2} < m < 0$) both f and f' are nonnegative for $s = +1$ and for all $\eta \geqslant 0$ (this also follows from the work of Ingham and Brown (1986)).
3. For $\gamma = 2$ and $s = +1$ (i.e. for $m = 1$) an elementary analytical upflow solution exists (see Section 5.1).
4. For $\gamma = \frac{2}{3}$ and $s = +1$ (i.e. for $m = -\frac{1}{3}$) a one-parameter family of exact analytical upflow solutions exists (see Section 5.2).
5. For $\gamma > 2$ and $s = +1$ (i.e. for $m > 1$) a second branch of upflow solutions exists. This result is also taken from Ingham and Brown (1986); see Sections 5.5 and 5.7).

It is worth underlining here that the analogy between the present upflow problem and the Cheng–Minkowycz problem is restricted to the mathematical aspects of corresponding boundary value problems for the self-similar stream function $f(\eta)$, but the physics underlying the equations is quite different due to the viscous dissipation effect. The dimensional velocity and temperature fields as expressed in terms of coordinates X and Y are also manifestly different in the present exponentially similar case (see Eqs. (13)–(15)) and the Cheng–Minkowycz power-law similarity case (Cheng and Minkowycz, 1977).

4.2. Downflows

In contrast to the upflow problem discussed above, in the case of the downflows, as given by Eq. (25) with $s = -1$, the previous literature on flow in porous media offers much less information. The only downflow solution known in closed analytical form is the ADP (see Section 5.6). We defer the detailed discussion of the downflow problem until Sections 6 and 7, only anticipating here that solutions of Eq. (16) exist for all positive values of γ ($m < -1$ and $s = -1$ in Eq. (25). The domains of existence of the up- and downflow solutions in the parameter plane (m, γ) are shown in Fig. 2.

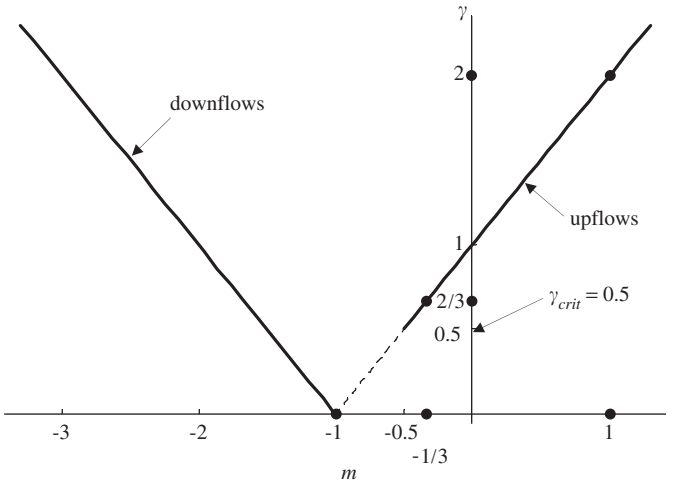

Fig. 2. Domains of existence of the up- and downflow solutions in the parameter plane (m, γ). The dots mark the exact up- and down flow solutions corresponding to the parameter values $(m, \gamma) = (1, 2)$, $(m, \gamma) = (-\frac{1}{3}, \frac{2}{3})$ and $(m, \gamma) = (-1, 0)$, respectively.

5. Solutions

5.1. Exact upflow solution for $\gamma = 2$

For $s = +1$ and the value $a = 2Ge$ of the temperature exponent the problem (16), (17) admits the elementary solution,

$$f(\eta) = 1 - \mathrm{e}^{-\eta}. \tag{27}$$

The corresponding temperature field (15), expressed in terms of the coordinates X and Y, is

$$T = T_\infty + T_0 \exp[2GeX - (GeRa)^{1/2}\mathrm{e}^{GeX}Y]. \tag{28}$$

The wall temperature gradient is given by $f''(0) = -1$.

The solution (27) is also known from the theory of boundary layer flows induced by continuous surfaces stretched with the linearly rising velocity $u_w \sim X$. It was first reported by Crane (1970).

5.2. Exact upflow solutions for $\gamma = 2/3$

As has been shown recently by Magyari et al. (2003), the boundary value problem which, in the present context, results from Eqs. (16) and (17) for $s = +1$ and $a = 2Ge/3$, admits a one-parameter family of solutions, one solution for every positive value of $f''(0)$. These solutions may be expressed in terms of Airy functions as follows:

$$f(\eta) = [36f''(0)]^{1/3}\frac{Bi'(z_0)Ai'(z) - Ai'(z_0)Bi'(z)}{Bi'(z_0)Ai(z) - Ai'(z_0)Bi(z)}, \tag{29}$$

$$f' = f''(0)\eta + 1 - \frac{1}{6}f^2, \tag{30}$$

where

$$z = [\sqrt{6}f''(0)]^{-2/3}(1 + f''(0)\eta), \quad z_0 = z|_{\eta=0}. \tag{31}$$

The far-field behaviour of this solution is

$$f(\eta) \to \sqrt{6 + 6f''(0)\eta} \quad \text{as} \quad \eta \to \infty \tag{32}$$

for all $f''(0) > 0$. Notice that $\lim_{\eta\to\infty} f(\eta)f'(\eta) = 3f''(0) > 0$ for these solutions, i.e. in this case, condition (21) and its consequences do not hold.

A remarkable feature of the solution (29) is that the algebraic asymptotic behaviour which it has when $f''(0) > 0$ is transformed into an exponential decay in the limit as $f''(0) \to 0$, when it may be described in terms of the well-known hyperbolic tangent solution. Indeed, by using the asymptotic properties of the Airy functions (see Abramowitz and Stegun (1965), for example) one obtains

$$f(\eta) \to (6+6f''(0)\eta)^{1/2} \tanh\left(\frac{(1 + f''(0)\eta)^{3/2} - 1}{(27/2)^{1/2} f''(0)}\right) \to \sqrt{6}\tanh\left(\frac{\eta}{\sqrt{6}}\right) \quad \text{as } f''(0) \to 0. \tag{33}$$

In this way one obtains $f'(\eta) = 1/\cosh^2(\eta/\sqrt{6})$ when $f''(0) = 0$, which shows that the family of solutions $f'(\eta)$ which exhibit *algebraic* decay of the form, $f'(\eta) \to 3f''(0)(6 + 6f''(0)\eta)^{-1/2}$ as $\eta \to \infty$, whenever $f''(0) > 0$, transforms into a solution which exhibits *exponential* asymptotic decay of the form, $f'(\eta) \to 4\exp(-2\eta/\sqrt{6})$ as $\eta \to \infty$. In the limit $f''(0) \to 0$. It is also worth noticing here that the form,

$$f(\eta) = \sqrt{6}\tanh(\eta/\sqrt{6}), \tag{34}$$

coincides with the free plane jet solution of Eq. (16) which was found almost 70 years ago by Bickley (1937). The wall heat flux (19) corresponding to the solution (34) is zero.

5.3. Ingham–Brown estimates (upflows)

Valuable analytical estimates for $f''(0)$ and $f(\infty)$ have been given by Ingham and Brown (1986) for $s = +1$ in the range, $0 < m + 0.5 \ll 1$ as well as for m close to zero. In the present context of the exponentially self-similar upflows, these estimates read

$$f''(0) = 0.078103\,(\gamma - \gamma_{\text{crit}})^{-3/4} \quad \text{and} \quad f(\infty) = 1.77828\,(\gamma - \gamma_{\text{crit}})^{-1/4} \tag{35}$$

for $0 < \gamma - \gamma_{\text{crit}} \ll 1$, and

$$f''(0) = -0.44375 - 0.85665\,(\gamma - 1) + 0.66943(\gamma - 1)^2 \tag{36}$$

for $|\gamma - 1| \ll 1$, respectively.

5.4. Banks estimates (upflows)

Banks (1983) performed a comprehensive analytical and numerical investigation of self-similar boundary layer flows induced in clear viscous fluids by continuous surfaces stretched with power-law velocities $u_w = U_0 X^m$. The boundary value problem he obtained,

$$F''' + FF'' - \frac{2m}{m+1}F'^2 = 0,$$
$$F(0) = 0, \quad F'(0) = 1, \quad F'(\infty) = 0 \tag{37}$$

for his self-similar stream function, $F = F(\xi)$, may be mapped onto the present problem (16), (17) by the transformation

$$m = s\gamma - 1, \quad \xi = \sqrt{\frac{\gamma}{2}}\,\eta,\ F(\xi) = \sqrt{\frac{\gamma}{2}}\,f(\eta). \tag{38}$$

In this way several of the numerical and analytical results of Banks (1983) may be applied to the present problem. Indeed, the transformation (38) yields the following expressions for $f''(0)$ and $f(\infty)$:

$$f''(0) = \sqrt{\frac{\gamma}{2}}\,F''(0) \quad \text{and} \quad f(\infty) = \sqrt{\frac{2}{\gamma}}\,F(\infty). \tag{39}$$

Thus, in the neighbourhood of the lower bound, $0 < \gamma - \gamma_{\text{crit}} \ll 1$, of the domain of existence of upflow solutions (see Fig. 2), the following estimates may be made:

$$f''(0) = 0.078102\,(\gamma - \gamma_{\text{crit}})^{-3/4}[1 - 3.22997\,(\gamma - \gamma_{\text{crit}})], \tag{40a}$$

$$f(\infty) = 1.77828\,(\gamma - \gamma_{\text{crit}})^{-1/4}[1 - 0.58772\,(\gamma - \gamma_{\text{crit}})]. \tag{40b}$$

Eqs. (35) and (40) are in excellent agreement with each other.

5.5. The second upflow solution branch

All the exact and approximate analytical solutions listed above (Eqs. (27)–(40)) belong to the same upflow solution branch of the boundary value problem (16), (17) which may be called the "first solution branch". In the parameter range $m > 1$ (which in the present case means $\gamma > 2$, $s = +1$), Ingham and Brown (1986) also found a second solution branch. The values of $f''(0)$ and $f(\infty)$ for $m \gg 1$ (i.e. for $\gamma \gg 1$ in the present case) may be determined from the results of Ingham and Brown (1986) and are

$$f''(0) = -0.90638\,(\gamma - 1)^{1/2}, \quad f(\infty) = 1.28077\,(\gamma - 1)^{-1/2} \tag{41}$$

for the first upflow solution branch, and

$$f''(0) = -0.91334\,(\gamma - 1)^{1/2}, \quad f(\infty) = 0.43365\,(\gamma - 1)^{-1/2} \tag{42}$$

for the second upflow branch.

On the first solution branch $f'(\eta) > 0$ holds for all values of η, but, for the second branch, there exists a value of η above which there exists negative values of $f'(\eta)$. Given that $f'(\eta)$ corresponds to the fluid temperature, this implies that second branch upflow solutions are unphysical since negative values of $f'(\eta)$ correspond to temperatures which are lower than the ambient temperature.

5.6. The ADP: an exact downflow solution for $\gamma = 0$

For $\gamma = 0$ (i.e. for $a = 0$) the boundary value problem given by Eqs. (16) and (17) admits an exact downflow solution. This is the ADP which was discovered recently by Magyari and Keller (2003) and Rees et al. (2003). It is given by,

$$f(\eta) = \eta\left(1 + \frac{\eta}{\sqrt{6}}\right)^{-1}, \quad f'(\eta) = \left(1 + \frac{\eta}{\sqrt{6}}\right)^{-2}, \tag{43}$$

where

$$f''(0) = -\sqrt{2/3} \quad \text{and} \quad f_\infty = \sqrt{6}. \tag{44}$$

In this case the exponential wall temperature distribution (1) reduces to a constant value, $T_w(x) = T_\infty - T_0$ and the wall is isothermal. The similarity variable η also becomes independent of the wall coordinate x, i.e. $\eta = (GeRa)^{1/2}Y$. Hence, the ADP is a strictly parallel flow for which the dimensional velocity and temperature fields, as given by Eqs. (13)–(15), are

$$u = \frac{\alpha}{L}Ra\left(1 + \sqrt{\frac{GeRa}{6}}Y\right)^{-2}, \quad v \equiv 0, \tag{45}$$

$$T = T_\infty - T_0\left(1 + \sqrt{\frac{GeRa}{6}}Y\right)^{-2}. \tag{46}$$

Using the ADP solution (43) one easily deduces from Eqs. (16) and (17) that the following analytical approximations must hold for small values of γ:

$$f''(0) = -\sqrt{\frac{2}{3(1-\gamma)}} \quad \text{and} \quad f(\infty) = \sqrt{6(1-\gamma)}, \quad (0 < \gamma \ll 1). \tag{47}$$

5.7. New analytical series solutions

The main difficulty encountered when solving two point boundary value problems of the type represented by Eqs. (16) and (17) is the ability to satisfy the boundary condition at infinity to a prescribed precision. The aim of the present section is to obtain an analytical series solution of the problem given by Eqs. (16) and (17) in a form which automatically satisfies the boundary condition $f'(\infty) = 0$ precisely. Clearly this requirement is not satisfied by a standard Taylor series expansion of $f(\eta)$ in powers of the similarity variable η (i.e. a Blasius series). However, the method of the Taylor expansion may be adapted easily to the present goal. Indeed, one of the most frequently used procedures for the solution of differential equations is the coordinate transformation. Therefore, we will introduce a suitable transformation $z = z(\eta)$ of the independent variable η and then look for the solution in the form of a power series of the new independent variable z,

$$f(\eta) = \sum_{n=0}^{\infty} A_n[z(\eta)]^n. \tag{48}$$

In the present context, "suitable" means that the boundary condition

$$f'(\infty) = \lim_{\eta\to\infty} \sum_{n=1}^{\infty} [n A_n z^{n-1}(\eta) z'(\eta)] = 0 \tag{49}$$

is satisfied precisely. There exists an infinite number of different variable transformations which satisfy the requirement, (49). If, for example, one wishes to recover the ADP given by Eq. (43) by this method, then $z = (1 + \text{const}\,\eta)^{-1}$ should be chosen. If, on the other hand, an algebraic behaviour of the form of Eq. (31) is suspected, then it is reasonable to choose $z = (1 + \text{const}\,\eta)^{-1/2}$ and to start the summation in Eq. (48) with $n = -1$ instead of $n = 0$. Finally, when one is interested in finding solutions with an exponential decay, similar to those of the exact solutions (27) and (34), then an exponential choice for z is reasonable. Obviously, one may also choose polynomials of exponentials of η, products of powers of η and exponentials of η, etc. In the present paper it is sufficient to proceed with the simple exponential *ansatz*

$$z = \mathrm{e}^{-b\eta}. \tag{50}$$

Here b is a positive constant which ensures that the condition $f'(\infty) = 0$ is satisfied automatically. Then, from Eqs. (48) and (50), $A_0 = \lim_{\eta\to\infty} f(\eta) \equiv f_\infty$ follows immediately, and we see that the free term of the series (48) is equal to the entrainment velocity f_∞. Furthermore, on substituting (48) and (50) into Eq. (16) and identifying the coefficients of like powers of z, then, for $n = 1$ we obtain,

$$b = \frac{\gamma f_\infty}{2}. \tag{51}$$

The assumption $b > 0$ implies, in agreement with our physical expectation, that the dimensionless entrainment velocity f_∞ is positive. The other coefficients of the expansion (48) may be written in terms of A_1 as follows:

$$A_k = \frac{\sum_{n=1}^{k-1} [n^2 - \beta n(k-n)] A_n A_{k-n}}{k^2(k-1) f_\infty}, \quad k = 2, 3, 4, \ldots, \tag{52}$$

where

$$\beta = 2\left(1 - \frac{s}{\gamma}\right) = \frac{2m}{m+1}. \tag{53}$$

Bearing in mind that both f_∞ and the coefficients A_k are not yet determined, it is convenient to eliminate f_∞ from the recurrence equations (52). This may be accomplished by substituting

$$A_k = \frac{(A_1)^k}{(f_\infty)^{k-1}} B_k, \quad k = 2, 3, 4, \ldots \tag{54}$$

into Eq. (52). Therefore we obtain

$$\begin{aligned} &B_1 = 1, \\ &B_k = \frac{\sum_{n=1}^{k-1} [n^2 - \beta n(k-n)] B_n B_{k-n}}{k^2(k-1)}, \quad k = 2, 3, 4, \ldots. \end{aligned} \tag{55}$$

These recurrence equations allow a rapid symbolical and numerical evaluation of the coefficients B_n for any given value of β. In order to be specific, we list below the analytical expressions of the first few B's:

$$
\begin{aligned}
B_1 &= 1,\\
B_2 &= +\frac{1-\beta}{4},\\
B_3 &= -\frac{1-\beta}{72}(4\beta-5),\\
B_4 &= +\frac{1-\beta}{1728}(21\beta^2-53\beta+34),\\
B_5 &= -\frac{1-\beta}{172800}(456\beta^3-1741\beta^2+2235\beta-968),\\
B_6 &= +\frac{1-\beta}{5184000}(2960\beta^4-15161\beta^3+29286\beta^2-25315\beta+8278).
\end{aligned}
\tag{56}
$$

Then, with the notations

$$
\frac{A_1}{f_\infty}=\lambda \quad \text{and} \quad B_0=1. \tag{57}
$$

Eq. (48) takes the form,

$$
f(\eta)=f_\infty\sum_{n=0}^{\infty}B_n\lambda^n\exp\left(-\frac{1}{2}n\gamma f_\infty\eta\right) \tag{58a}
$$

and the boundary condition $f(0)=0$ becomes

$$
G(\lambda)\equiv\sum_{n=0}^{\infty}B_n\lambda^n=0. \tag{59a}
$$

The coefficients B_k, which are given by Eqs. (55), depend only on the parameter β (i.e. on s/γ, according to Eq. (53). Thus, once the parameter λ is determined as a solution of Eq. (59a), Eq. (58a) yields the formal solution of the boundary value problem (16), (17) in terms of the dimensionless entrainment velocity f_∞. For this latter quantity, the boundary condition $f'(0)=1$ and Eq. (58a) yield the expression

$$
f_\infty=\left(-\frac{\gamma}{2}\sum_{n=0}^{\infty}nB_n\lambda^n\right)^{-1/2}. \tag{60a}
$$

The wall temperature gradient $f''(0)$ may be written as

$$
f''(0)=f_\infty^3\left(\frac{\gamma}{2}\right)^2\sum_{n=0}^{\infty}n^2\lambda^nB_n. \tag{61a}
$$

The rate of convergence of the series occurring in Eqs. (58a)–(61a) can be accelerated with the aid of Euler's series transformation (see, for example, Abramowitz and Stegun, 1965). On using an alternative

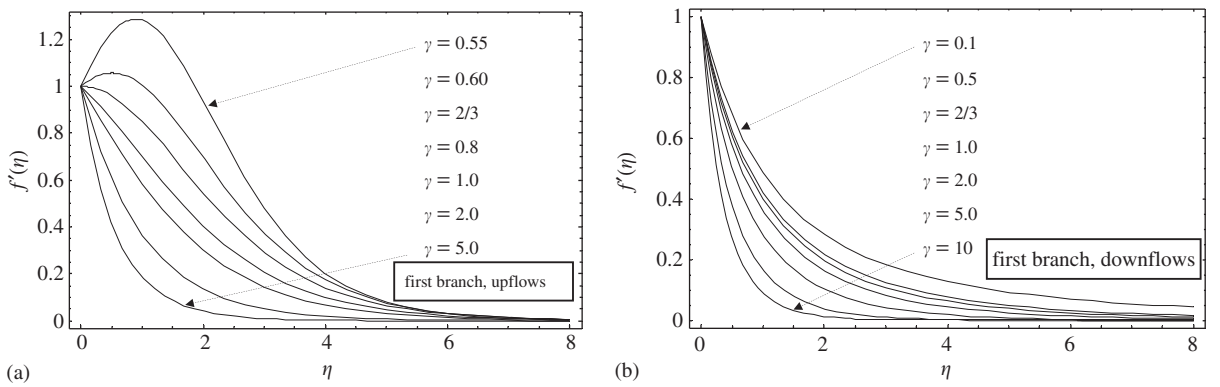

Fig. 3. (a). Upflow velocity (and temperature) profiles corresponding to different values of the parameter $\gamma = a/Ge$ (first solution branch). (b). Downflow velocity (and temperature) profiles corresponding to different values of the parameter $\gamma = a/Ge$ (first solution branch).

form of this transformation which is due to Knopp (1990), Eqs. (58a)–(61a) may be rewritten as follows:

$$f(\eta) = \frac{f_\infty}{2} \sum_{k=0}^{\infty} \left[\frac{k!}{2^k} \sum_{n=0}^{k} \frac{B_n \lambda^n}{(k-n)!n!} \exp\left(-\frac{1}{2} n \gamma f_\infty \eta \right) \right], \tag{58b}$$

$$G(\lambda) \equiv \sum_{k=0}^{\infty} \left(\frac{k!}{2^k} \sum_{n=0}^{k} \frac{B_n \lambda^n}{(k-n)!n!} \right) = 0, \tag{59b}$$

$$f_\infty = \left[-\frac{\gamma}{4} \sum_{k=0}^{\infty} \left(\frac{k!}{2^k} \sum_{n=0}^{k} \frac{n B_n \lambda^n}{(k-n)!n!} \right) \right]^{-1/2}, \tag{60b}$$

$$f''(0) = \frac{f_\infty^3}{2} \left(\frac{\gamma}{2} \right)^2 \sum_{k=0}^{\infty} \left(\frac{k!}{2^k} \sum_{n=0}^{k} \frac{n^2 B_n \lambda^n}{(k-n)!n!} \right). \tag{61b}$$

As a first simple example we show that the exact upflow solution (27) corresponding to $\gamma = 2$ and $s = +1$ can be recovered immediately from the above equations. Indeed, in this case, $\beta = 1$ and from Eqs. (56) we obtain $B_1 = 1$, $B_k = 0$, $k = 2, 3, 4, \ldots$. Thus, Eq. (59a) becomes $1 + \lambda = 0$ and yields $\lambda = -1$. Then, Eqs. (60a) and (61a) give $f_\infty = 1$ and $f''(0) = -1$, respectively. Finally, from Eq. (58a), we recover the exact solution (27).

The exact solution (34) corresponding to $\gamma = \frac{2}{3}$, may also be recovered by the numerical evaluation of Eqs. (58b)–(61b). It may also be recovered analytically but some special summation methods of asymptotic series are required (e.g. the Borel summation).

We have collected a large number of up- and downflow first branch solutions in Table 1. As an illustration of some of these, Figs. 3a and b display a couple of upflow and downflow velocity (temperature) profiles, $f'(\eta)$, corresponding to different values of the parameter $\gamma = a/Ge$. All the data contained in Table 1 has been obtained by using Eqs. (58a)–(61a) or Eqs. (58b)–(61b), except for the upflow solution corresponding to $\gamma = 0.51$ which has been calculated numerically with the aid of a Runge–Kutta method and the shooting

Table 1
The values of $f''(0)$ and $f(\infty)$ for the *first branch* of upflow (hot plate, $s=+1$) and downflow (cold plate, $s=-1$) solutions

$\gamma=\frac{a}{Ge}$	First solution branch			
	Upflows (hot plate, $s=+1$)		Downflows (cold plate, $s=-1$)	
	$f''(0)$	$f(\infty)$	$f''(0)$	$f(\infty)$
0	For $0<\gamma\leqslant\gamma_{\text{crit}}=0.5$ no upflow solutions exist		$-0.816=-\sqrt{2/3}^{*}$	$2.449=\sqrt{6}^{*}$
0.05			−0.840669	2.171736
0.1			−0.864227	2.005790
0.2			−0.909662	1.778382
0.3			−0.953085	1.620144
0.4			−0.994726	1.499964
0.5			−1.034775	1.404076
0.51	2.417131	5.564696	−1.038699	1.395505
0.55	0.597658	3.587188	−1.054254	1.362774
0.6	0.221094	2.903538	−1.073393	1.325018
$\frac{2}{3}$	0^{*}	$\sqrt{6}^{*}$	−1.098412	1.279353
0.8	−0.234256	1.978203	−1.146864	1.200857
1	−0.443748	1.616125	−1.216019	1.106547
1.5	−0.770368	1.201224	−1.374023	0.943446
2	-1^{*}	1^{*}	−1.515834	0.836421
3	−1.348454	0.787736	−1.765830	0.700107
4	−1.624356	0.670850	−1.984701	0.614244
5	−1.859928	0.594213	−2.181776	0.553811
6	−2.068913	0.539000	−2.362494	0.508307
7	−2.258674	0.496785	−2.530352	0.472448
8	−2.433700	0.463156	−2.687757	0.443247
9	−2.596968	0.435546	−2.836446	0.418868
10	−2.750568	0.412351	−2.977724	0.398115
50	−6.358095	0.181769	−6.459622	0.180497
100	−9.027795	0.128303	−9.099584	0.127853
500	−20.251115	0.057298	−20.283219	0.057258
1000	−28.650758	0.040509	−28.673459	0.040494

The superscript * indicates the exact solutions discussed in Sections 5.1 and 5.2.

method. The reason for using the direct numerical solution is that when $s=+1$ and γ is close to its critical value, $\gamma_{\text{crit}}=0.5$ (i.e. $\beta=-2^{+}$, $m=-0.5^{+}$), is that both the series in (59a) and (59b) become divergent and thus no root of Eqs. (59a) and (59b) could be determined reliably in this neighbourhood. In all other cases included in Table 1 the solution λ corresponding to the *first branch* of both up- and downflow solutions of Eq. (59a) or (59b) have been calculated by increasing the number of terms of the sum taken into account, until the results for $f''(0)$ and $f(\infty)$ remained unchanged in the sixth decimal digit. On comparing the "exact" data of Table 1 with the approximate values obtained from the corresponding Ingham–Brown and Banks estimates discussed in Sections 5.3–5.5, an excellent agreement has been found. Furthermore, on using the data of Table 1, Fig. 4a shows the wall temperature gradient $f''(0)$ as function of γ for the *first branch* of both upflow and downflow solutions. Similarly, on using the data of Tables 2 and 3, in Fig. 4b $f''(0)$ is plotted for up- and downflows of the *second solution branch* (for a detailed physical discussion of these and of the subsequent results of the present section see Sections 6 and 7).

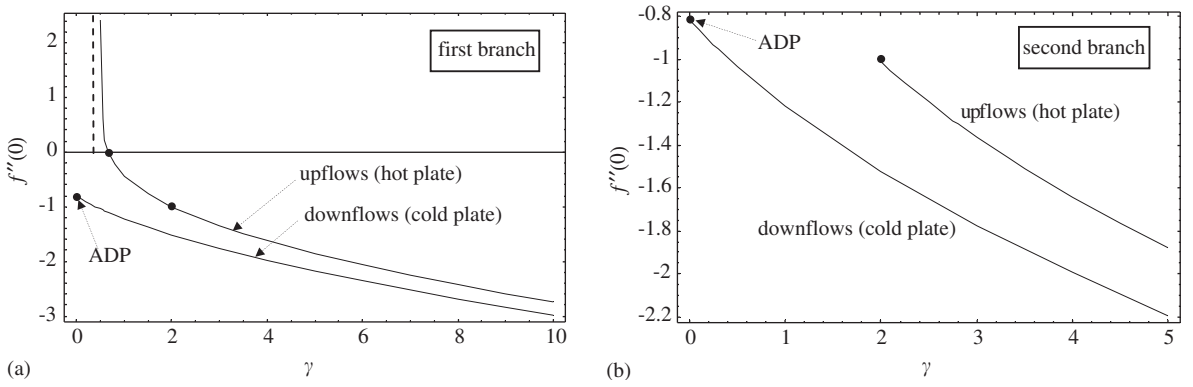

Fig. 4. (a). Plot of $f''(0)$ as a function of γ for the *first branch* of up- and downflow solutions. The positive and negative values of $-s\,f''(0)$ correspond to a direct ($q_w > 0$) and a reverse ($q_w < 0$) wall heat flux, respectively. The wall heat flux is always negative for downflow cases (cold plate, $s = -1$), as expected, but, for upflows (hot plate, $s = +1$) it is positive above the value $\gamma = \frac{2}{3}$ and becomes reversed when $\gamma_{\text{crit}} = 0.5 < \gamma < \frac{2}{3}$. The dots correspond to the values $\gamma = 0$, $\gamma = \frac{2}{3}$ and $\gamma = 2$ for which exact solutions exist (see Sections 5.1, 5.3 and 5.6) and the dashed vertical asymptote corresponds to $\gamma_{\text{crit}} = 0.5$. For large values of γ, both of the plotted curves scale with $\sqrt{\gamma}$ such that $-s\,f''(0)/\sqrt{\gamma} \to 0.906376$ as $\gamma \to \infty$ (see also Fig. 11a). (b). Plot of $f''(0)$ as a function of γ for the *second branch* of upflow and downflow solutions. The positive and negative values of $-s\,f''(0)$ correspond to a direct ($q_w > 0$) and a reverse ($q_w < 0$) wall heat flux, respectively. The wall heat flux is again negative for downflow cases (cold plate, $s = -1$), as expected, and positive for the upflows (hot plate, $s = +1$). The dots correspond to the values $\gamma = 0$, $\gamma = \frac{2}{3}$ and 2 for which exact solutions exist (see Sections 5.1, 5.3 and 5.6) and the dashed vertical asymptote corresponds to $\gamma_{\text{crit}} = 0.5$. For large values of γ, both of the plotted curves scale with $\sqrt{\gamma}$ such that $-s\,f''(0)/\sqrt{\gamma} \to 0.906376$ as $\gamma \to \infty$ (see also Fig. 11b).

Table 2
The values of $f''(0)$ and $f(\infty)$ for the *first* and *second upflow branches* for $2.01 \leqslant \gamma \leqslant 5$

$\gamma = \frac{a}{Ge}$	Upflows (hot plate, $s = +1$)			
	First branch		Second branch	
	$f''(0)$	$f(\infty)$	$f''(0)$	$f(\infty)$
2.01	−1.004072	0.996951	−1.014102	0.076913
2.05	−1.020202	0.985029	−1.031700	0.097938
2.1	−1.040020	0.970714	−1.052321	0.111512
2.25	−1.097370	0.931264	−1.110902	0.134444
2.5	−1.186906	0.875047	−1.201483	0.153283
2.75	−1.270224	0.827948	−1.285466	0.162536
3	−1.348454	0.787736	−1.364213	0.167161
3.5	−1.492755	0.722281	−1.509359	0.169668
4	−1.624356	0.670850	−1.641694	0.168059
4.5	−1.746106	0.629053	−1.764125	0.164796
5	−1.859928	0.594213	−1.878595	0.160892

The present approach also allows us to calculate the second branch of upflow solutions which, as predicted by Ingham and Brown (1986), arise in the parameter range $\gamma > 2$ (i.e. for $m > 1$). The results obtained for a set of values of γ in the range $2.01 \leqslant \gamma \leqslant 5$ are displayed in Table 2 and the corresponding

Table 3
The values of $f''(0)$ and $f(\infty)$ for the *first* and *second downflow branches* for $0 \leqslant \gamma \leqslant 2$

$\gamma = \frac{a}{Ge}$	Downflows (cold plate, $s = -1$)			
	First branch		Second branch	
	$f''(0)$	$f(\infty)$	$f''(0)$	$f(\infty)$
0	$-0.816 = \sqrt{2/3}^*$	$2.449 = \sqrt{6}^*$	$-.816 = -\sqrt{2/3}^*$	$2.449 = \sqrt{6}^*$
0.1	−0.864227	2.005790	−0.864230	1.743320
0.25	−0.931609	1.693211	−0.931729	1.269554
0.3	−0.953085	1.620144	−0.953289	1.168985
0.5	−1.034775	1.404076	−1.035503	0.898282
1	−1.216019	1.106547	−1.218553	0.593499
2	−1.515834	0.836421	−1.521744	0.381991
3	−1.348454	0.787736	−1.774423	0.296144
4	−1.624356	0.670850	−1.995515	0.248361
5	−1.859928	0.594213	−2.194505	0.217362

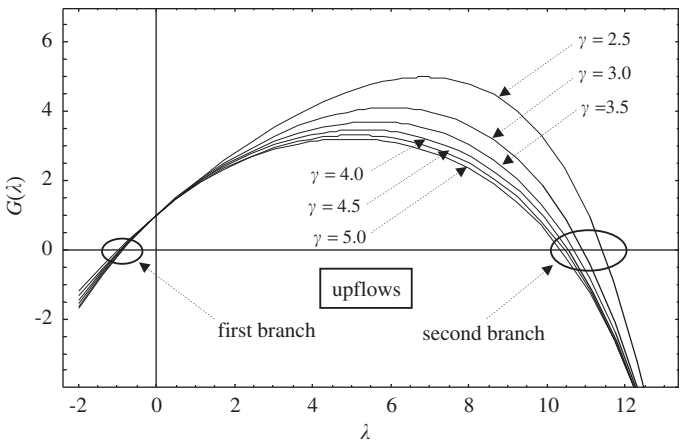

Fig. 5. The zeros of Eq. (56) in the neighbourhood of $\lambda = -1$ correspond to the *first branch* of upflow solutions and those between the values 10 and 12 of λ to the *second branch* of upflow solutions for the specified γ -values. The corresponding values of $f''(0)$ and $f(\infty)$ shown in Table 2.

solutions illustrated in Figs. 5 and 6. In this range Eqs. (59a) and (59b) have two distinct roots λ for any specified value of γ, and these correspond to the first and second branch of the upflow solutions, as shown in Fig. 5.

Concerning these two solution branches, a remarkable detail is that they do not just represent two isolated solutions, as one has believed until now, but they also form the limiting cases of a family of nondenumerable multiple solutions. This circumstance is illustrated in Fig. 7 for $\gamma = 5$. The solutions corresponding to the values $f''_{\text{first}}(0)$ and $f''_{\text{second}}(0)$ of $f''(0)$ represent the upper and lower bound of

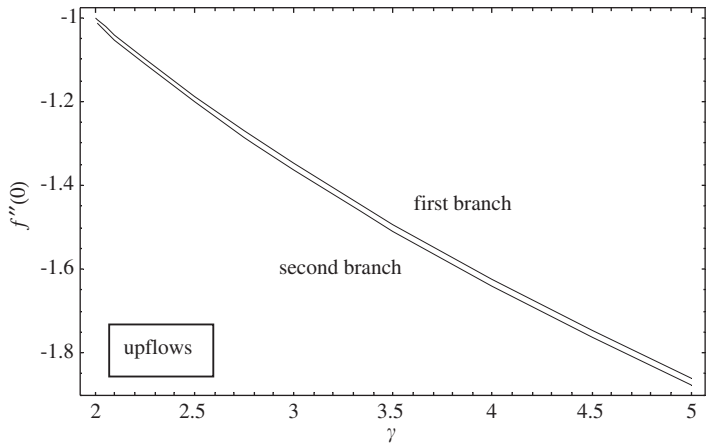

Fig. 6. Plot of $f''(0)$ as function of γ for the *first* and *second upflow branches* for $2 \leqslant \gamma \leqslant 5$. The values of the (direct) wall heat fluxes in the two cases are quite close to each other.

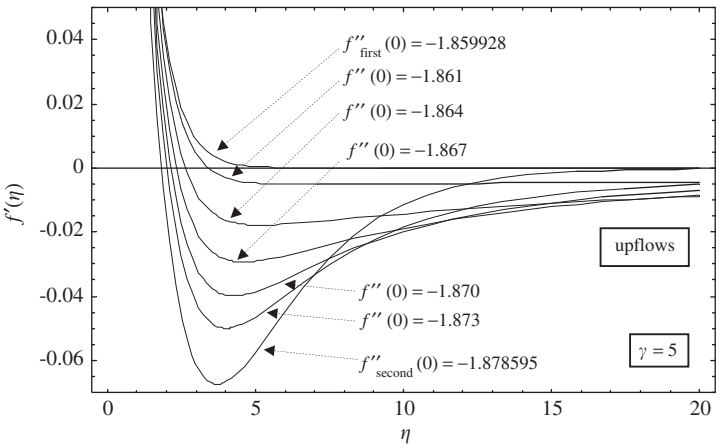

Fig. 7. Velocity (and temperature) profiles for the values of $f''(0)$ corresponding to the first and second upflow branches (according to the last row of Table 2) and for a selection of values of $f''(0)$ lying between $f''_{\text{first}}(0)$ and $f''_{\text{second}}(0)$ for $\gamma = 5$. The solutions corresponding to the values $f''_{\text{first}}(0)$ and $f''_{\text{second}}(0)$ of $f''(0)$ represent, respectively, the upper and lower bounds of a family of nondenumerable multiple solutions.

this family of multiple upflow solutions, respectively (see Table 2). It must be noted, however, that the presence of this family of solutions does not contradict the fact that the two bounding cases correspond to the only two roots for λ shown in Fig. 5. The two roots correspond to exponentially decaying solutions, whereas the family of solutions decay algebraically, and therefore the curve shown in Fig. 5 does not apply to these solutions.

A further interesting new result is the existence of a second branch of solutions for downflows. The results obtained for a couple of values of γ in the range $0 \leqslant \gamma \leqslant 2$ are collected in Table 3 and illustrated in Fig. 8. However, in this range of values of γ, the series (56a,b) converge only for the first branch. The second

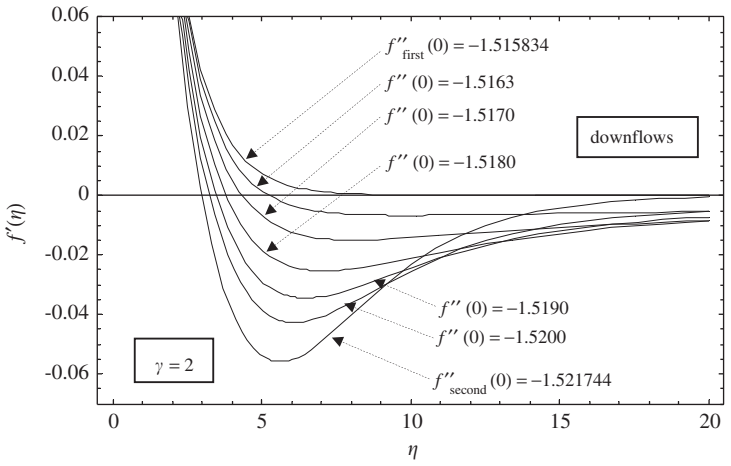

Fig. 8. Velocity profiles for the values of $f''(0)$ corresponding to the first and second downflow branches (according to the last row of Table 3) and for a selection of values of $f''(0)$ lying between $f''_{\text{first}}(0)$ and $f''_{\text{second}}(0)$ for $\gamma = 2$. The solutions corresponding to the values $f''_{\text{first}}(0)$ and $f''_{\text{second}}(0)$ of $f''(0)$ represent, respectively, the upper and lower bounds of a family of nondenumerable multiple solutions.

branch of downflows has been calculated numerically using the shooting method. In contrast to the second branch of upflow solutions, the second branch of downflow solutions are physically meaningful solutions of the present problem (see further details in Section 7). As with their upflow counterparts plotted in Fig. 7, the two downflow solution branches also represent the bounding cases of a family of nondenumerable multiple solutions, see Fig. 8. The solutions corresponding to the values $f''_{\text{first}}(0)$ and $f''_{\text{second}}(0)$ of $f''(0)$ again represent the upper and lower bounds of this family of multiple downflow solutions, respectively (see Table 3). Figs. 7 and 8 show that, while the two "branches" are rapidly decaying solutions, the intermediate solutions decay slowly as $\eta \to \infty$. This difference in the asymptotic behaviour of the $f'(\eta)$ -profiles shown in Figs. 7 and 8 becomes greater in the case of the corresponding stream functions $f(\eta)$. The downflows of Fig. 8 are illustrated in Fig. 9 which shows, that while the entrainment velocities $f(\infty)$ of the two solution branches are finite and nonzero (see Table 3), $f(\infty)$ for the intermediate solutions enclosed between the branches is zero. In the γ-ranges included in Tables 2 and 3, the values of the wall temperature gradient $f''(0)$ for the two respective solution branches are quite close to each other. However, the values of $f(\infty)$ for the two respective solution branches differ substantially from each other. This circumstance is illustrated for the downflow cases of Table 3 by the plots shown in Fig. 10.

6. Effect of the viscous dissipation on the heat transfer

The effect of viscous dissipation on the wall heat transfer as a function of the parameter $\gamma = a/Ge$ is of great interest. In the present section it will be compared with the limiting case $Ge \to 0$ (i.e. $\gamma \to \infty$) which corresponds to negligible viscous dissipation (see Eq. (8)). To this end, we define the Nusselt

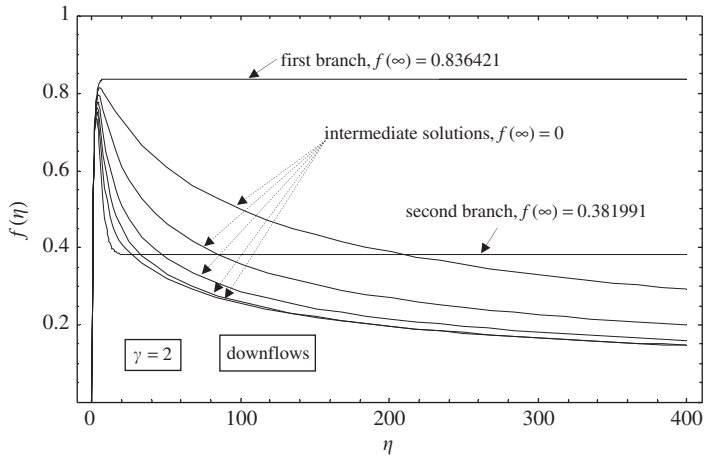

Fig. 9. Profiles of the stream function for the first and second downflow branches and for some of the intermediate profiles plotted in Fig. 8. For the two "branches" $f(\infty)$ is finite, while it is zero for the intermediate cases.

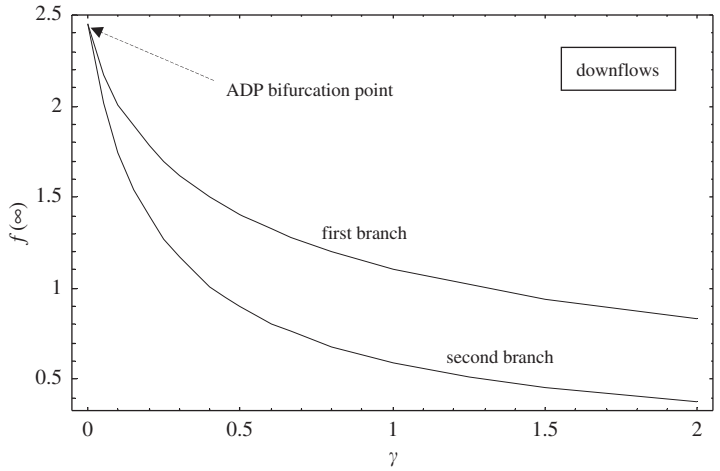

Fig. 10. Plot of $f(\infty)$ as function of γ for the *first* and *second downflow branches* for $0 \leqslant \gamma \leqslant 2$. The two downflow solutions branches bifurcate from the ADP corresponding to $\gamma = 2$.

number following the expression (19) for the wall heat flux:

$$Nu(\gamma) = -s\frac{f''(0)}{\sqrt{\gamma}}. \tag{62a}$$

For more transparency, the dependence on γ has been shown explicitly. Thus, Eqs. (61b) and (60b) yield

$$Nu(\gamma) = -s\left(-\sum_{k=0}^{\infty}\frac{k!}{2^k}\sum_{n=0}^{k}\frac{nB_n\lambda^n}{(k-n)!n!}\right)^{-3/2}\sum_{k=0}^{\infty}\left(\frac{k!}{2^k}\sum_{n=0}^{k}\frac{n^2B_n\lambda^n}{(k-n)!n!}\right), \tag{62b}$$

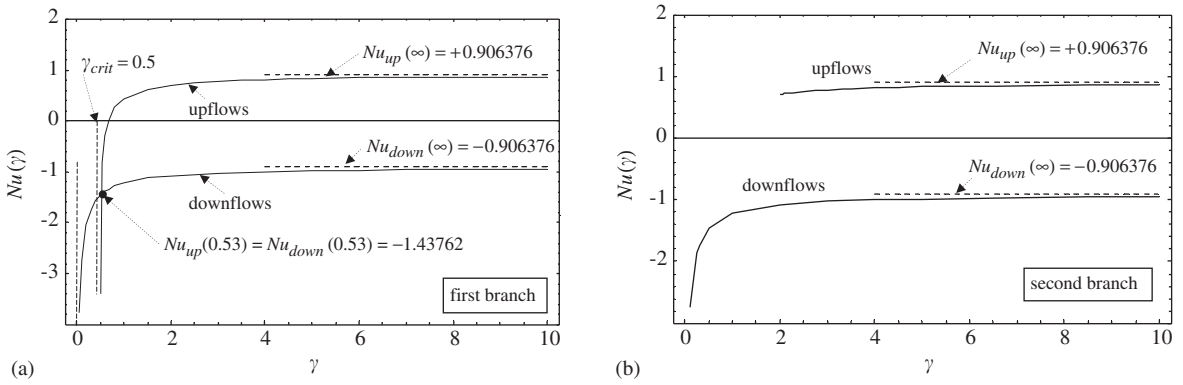

Fig. 11. (a). Plot of $Nu(\gamma)$ for the *first branch* of upflow and downflow solutions, respectively. For the downflows the Nusselt number is negative for all values of γ, whereas, in the case of upflows, it is positive above the value $\gamma = \frac{2}{3}$ and becomes negative in the range $\gamma_{\rm crit} = 0.5 < \gamma < \frac{2}{3}$. For $\gamma = 0.53$, the two Nusselt numbers are equal, $Nu_{\rm up}(0.53) = Nu_{\rm down}(0.53) = -1.43762$. In the absence of viscous dissipation ($Ge = 0$), i.e. for $\gamma \to \infty$, the up- and downflows become physically equivalent, and the absolute values of corresponding Nusselt numbers become equal. (b). Plot of $Nu(\gamma)$ for the *second branch* of up- and downflow solutions, respectively. For the downflows the Nusselt number is negative for all values of γ, whereas, in the case of upflows, it is positive in the whole existence domain $\gamma > 2$. In this case the two curves do not intersect each other. In the absence of viscous dissipation ($Ge = 0$), i.e. for $\gamma \to \infty$, the up- and downflows become physically equivalent, and the absolute values of corresponding Nusselt numbers become equal.

where the coefficients B_n and thus also the solution(s) λ of Eq. (59b) are functions of γ via β given by Eq. (53). As $Ge \to 0$ (i.e. $\gamma \to \infty$), Eq. (53) yields the common value $\beta = 2$ for both upflows and downflows, which is in agreement with the fact that, in the absence of viscous dissipation, upflows and downflows are physically equivalent. Moreover, for this value of β, Eq. (59b) has two solutions $\lambda_1 = -0.810275$ and $\lambda_2 = +9.786662$ which correspond to the first and second branch of solutions, respectively. For the corresponding Nusselt numbers one obtains

$$Nu_{\rm up}(\infty) = -Nu_{\rm down}(\infty) = 0.906376 \tag{63}$$

for the first and

$$Nu_{\rm up}(\infty) = -Nu_{\rm down}(\infty) = 0.910397 \tag{64}$$

for the second branch of solutions, respectively. (Notice that through $|Nu_{\rm up}(\infty)| = |Nu_{\rm down}(\infty)| = 0.906376$ the physical equivalence of the up- and downflows in the absence of viscous dissipation becomes manifest again.) The results (63) and (64) are in a good agreement with the results (41) and (42) of Ingham and Brown (1986). The connection of $Nu(\gamma)$ to its asymptotic values (63) for the first branch of up- and downflow solutions is illustrated by the plots of Fig. 11a (with discussion in Section 7). The corresponding curves for the second branch of solutions (shown in Fig. 11b) are very close to those of Fig. 11a since the values of $f''(0)$ itself for the first and second branch solutions are (in the corresponding domains of existence, $\gamma > 2$ for the first and $\gamma \geqslant 0$ for the second branch) quite close to each other (see Tables 2 and 3).

7. Discussion and conclusions

The investigation of free convection flow over a vertical plate with an exponential temperature distribution is motivated by the fact that, in contrast to the more familiar power-law temperature distributions, a similarity-reduction of the governing equations still remains possible even when the extra nonlinear effect of viscous dissipation is taken into account. This holds both for the viscous flow of clear fluids as well as for the flow in saturated porous media. Hence the influence of the viscous friction on the mechanical and thermal characteristics of the flow can be examined for the exponential-similarity case by exact analytical and numerical methods.

The main issues of the present paper are itemized below, and some of their consequences will be emphasized.

1. As an effect of heat release by viscous friction, the usual physical equivalence of the free convection up- and downflows over an upward projecting hot plate and over its downward projecting cold counterpart, respectively, gets broken (this statement holds both for the viscous flow of clear fluids and for the flow in saturated porous media). Accordingly, the possible delivery of useful work (exergy) by the two types of free convection flows is quite different.
2. A further important consequences of this "broken equivalence" is that (in the present problem) the downflows are possible for all nonnegative values of the temperature exponent a, but the upflows only can exist above a critical value of a, $a > a_{\mathrm{crit}} = Ge/2$ (Fig. 2). In other words, for the occurrence of an exponentially self-similar upflow, the logarithmic increment (6) of the wall temperature must be sufficiently large. The physical reason for this difference between the up- and downflow cases is that, while in the latter case the direction of motion coincides with the direction of the body force, in the former one it is opposite to this.
3. The Gebhart number Ge of the fluid plays an important role for all these free convection flows since the exponential dependence of the velocity and temperature fields on the wall coordinate x scales with Ge (see Eqs. (12)–(18)).
4. Eq. (16) of the present boundary value problem can be mapped by the substitution (24) on to Eq. (25). For upflow this equation coincides with the Cheng–Minkowycz equation which is valid for a plate with a power-law temperature distribution, $T_w(x) = T_\infty + T_0\, X^m$ when the effect of viscous dissipation is neglected. However, in the case of downflows, Eq. (25) differs from the Cheng–Minkowycz equation essentially. Accordingly, with respect to the Cheng–Minkowycz theory, the present downflow solutions are novel.
5. For the values $a = 2Ge$ and $a = 2Ge/3$ of the temperature exponent, analytical upflow solutions are available (see Sections 5.1 and 5.2). For the downflows a single analytical closed form solution is known. It is the ADP ((43) corresponding to $a = 0$ (i.e. an isothermal, downward projecting cold plate).
6. The upflow case corresponding to $a = 2Ge/3$ reveals a remarkable feature of the present boundary value problem. It shows that a "usual" exponentially decaying boundary layer solution arises here as a limiting case of a family of algebraically decaying solutions. This explicit example bridges the historical disagreement concerning the feasibility of exponentially and algebraically decaying boundary layers (see Kuiken, 1981; Magyari and Keller, 2004).
7. In Section 5.7 of the paper a new analytical series-solution in terms of powers of exponentials has been given. This approach allows the calculation of all the upflow and downflow solutions

belonging to the first branch (Tables 1–3, Figs. 2–4a, and 5–11a). The second solution branch of the Cheng–Minkowycz equation (for upflows) could also be recovered with this method (Table 2, Figs. 2, 4b, 5–7 and 11b).

8. In addition to the first branch of downflow solutions (Tables 1 and 3, Figs. 2, 3b, 4a, 8–11a), a second solution branch of downflow solutions has also been found (Table 3, Figs. 2, 4b, 8–11b). These two downflow solution branches bifurcate from the ADP at $a = 0$ and exist for all positive values of a.
9. It has been shown that the two solution branches do not represent in fact two isolated solutions but, in both upflow and downflow cases, they are the limiting cases of respective families of nondenumerable multiple solutions which are bounded between these branches (Figs. 7 and 8). As suggested by Figs. 7 and 8 the intermediate solutions decay algebraically as $\eta \to \infty$, while the two branches correspond to exponentially decaying solutions. Moreover, while the entrainment velocities $f(\infty)$ of the two branches are finite and nonzero, the intermediate solutions yield $f(\infty) = 0$ (see Fig. 9).
10. In the present context the second branch of upflow solutions are nonphysical since they lead to fluid temperatures which are (in spite of heat released by viscous friction) smaller than the ambient temperature T_∞. The second branch of downflow solutions, in contrast, are in agreement with the principles of thermodynamics. Indeed, in this case the lowest temperature is the wall temperature. Hence, negative values of $f'(\eta)$ arising in the second downflow solution branch are compatible with this requirement. Moreover, for the first branch of downflow solutions the inequality $0 < f'(\eta) < 1$ must hold for all $0 < \eta < \infty$. This is actually the case (see Fig. 3b).
11. The heat transfer characteristics of first branch of both up- and downflow solutions can easily be extracted from Figs. 4a and 11a. [Remember that the latter figure is a rescaled form of the former one, according to Eq. (62a).] Furthermore, the corresponding curves for the second branch of solutions are very close to those of Figs. 4a and 11a since the values of $f''(0)$ itself for the first and second branch solutions are, in the corresponding domains of existence, $\gamma > 2$ for the first and $\gamma \geqslant 0$ for the second branch, quite close to each other (see Tables 2 and 3 and Figs. 4b and 11b). Although the wall heat flux is always negative for downflows, in the case of upflows it is positive only above of the value $\gamma = \frac{2}{3}$ and, surprisingly, in spite of the hot wall, it becomes negative for $0.5 < \gamma < \frac{2}{3}$. The reason for this inversion of the heat fluxes at relatively low values ($Ge/2 < a < 2Ge/3$) of the wall temperature exponent a is due to the excess heat released in the bulk of the fluid by viscous dissipation. For large values of the logarithmic increment a, the heat released by viscous dissipation is no longer able to overcome the heat flux issuing from the hot wall. As seen in Fig. 11a, $Nu_{\mathrm{up}}(\gamma) < Nu_{\mathrm{up}}(\infty) = 0.906376$, which means that in the case of the upflows, the heat released by viscous dissipation decreases the heat transfer from the fluid to the hot wall for all values of the parameter $\gamma = a/Ge$. On the other hand, $Nu_{\mathrm{down}}(\gamma) < Nu_{\mathrm{down}}(\infty) = -0.906376$, which means that in the case of the downflows, the heat released by viscous dissipation increases the amount of heattransferred from the fluid to the cold wall. Both these effects of viscous dissipation are in agreement with our physical expectation.
12. Finally, it is also worth mentioning here that an expansion of type (48), (50) with respect to an "exponential base" also has been used recently by Liao and Pop (2003) in their investigation of the Cheng–Minkowycz problem with the aid of the homotopy analysis method (Liao, 2004). The method of Liao is based on a continuous variation of the base functions to the exact solution with the aid of auxiliary deformation operators, which also involves an auxiliary parameter which controls the convergence of the expansion. However, as reported by Liao and Pop (2003), the second branch of solutions of the Cheng–Minkowycz equation could not be recovered by the homotopy

Table 4
Hints for finding the different results of the present paper

Flow direction	Domain of existence, tables and figures	
	First branch	Second branch
Upflows (hot plate, $s = +1$, Fig. 1a)	$\gamma > \gamma_{\text{crit}} = 0.5$ Tables 1 and 2, Figs. 2, 3a, 4a, 5–7, and 11a	$\gamma > 2$ Tables 2, Figs. 2, 4b, 5–7, and 11b
Downflows (cold plate, $s = -1$, Fig. 1b)	$\gamma \geqslant 0$ Tables 1 and 3, Figs. 2, 3b, 4a, 8–11a	$\gamma \geqslant 0$ Tables 3, Figs. 2, 4b, 8–11b

analysis method. This circumstance and the results of the present paper suggest that in order to be converted to the exact solution, the exponential base, especially when combined with Euler's convergence accelerating series transformation, does not need any deformation for almost all values of the parameters γ and s.

The results of the present paper may be classified according to a 2×2 matrix which consist of the rows upflows, downflows and the columns first and second solution branches, respectively. This is shown in Table 4 where the domains of existence of the solutions as well as the numbers of tables and figures with the corresponding results have been compiled.

References

Abramowitz, M., Stegun, I.A., 1965. Handbook of Mathematical Functions. Dover Publ., Inc., New York.
Banks, W.H.H., 1983. Similarity solutions of the boundary layer equations for a stretching wall. J. Méc. Theor. Appl. 2, 375–392.
Bejan, A., 1995. Convection Heat Transfer. 2nd ed. Wiley, New York.
Bejan, A., Dincer, I., Lorente, S., Miguel, A.F., Reis, A.H., 2004. Porous and Complex Flow Structures in Modern Technologies. Springer, New York.
Bickley, W.B., 1937. The plane jet. Phil. Mag. 23, 727–731.
Cheng, P., Minkowycz, W.J., 1977. Free convection about a vertical flat plate embedded in a porous medium with application to heat transfer from a dike. J. Geophys. Res. 82, 2040–2044.
Crane, L.J., 1970. Flow past a stretching plate. J. Appl. Math. Phys. (ZAMP) 21, 645–647.
Gebhart, B., Mollendorf, J., 1969. Viscous dissipation in external natural convection flows. J. Fluid Mech. 38, 97–107.
Goldstein, S., 1939. A note on the boundary layer equations. Proc. Cambr. Phil. Soc. 35, 338–340.
Ingham, D.B., Brown, S.N., 1986. Flow past a suddenly heated vertical plate in a porous medium. Proc. Roy. Soc. London A 403, 51–80.
Knopp, K., 1990. Theory and Application of Infinite Series. Dover, New York.
Kuiken, H.K., 1981. On boundary layers in fluid mechanics that decay algebraically along stretches of wall that are not vanishingly small. IMA J. Appl. Math. 27, 387–405.
Liao, S.-J., 2004. Beyond Perturbation: Introduction to the Homotopy Analysis Method. Chapman & Hall/CRC Press, Boca Raton.
Liao, S.-J., Pop, I., 2003. Explicit analytic solution for similar boundary layer equations. Int. J. Heat Mass Transfer 47, 75–85.
Magyari, E., Keller, B., 2003. The opposing effect of viscous dissipation allows for a parallel free convection boundary layer flow along a cold vertical flat plate. Transport Porous Media 51, 227–230.
Magyari, E., Keller, B., 2004. Backward free convection boundary layers in porous media. Transport Porous Media 55, 285–300.

Magyari, E., Pop, I., Keller, B., 2003. New analytical solutions of a well known boundary value problem in fluid mechanics. Fluid Dyn. Res. 33, 313–317.

Nakayama, A., Pop, I., 1989. Free convection over a nonisothermal body in a porous medium with viscous dissipation. Int. Comm. Heat Mass Transfer 16, 173–180.

Nield, D.A., Bejan, A., 1999. Convection in Porous Media. 2nd ed.. Springer, New York.

Oberlack, M., 2000. Symmetrie, Invarianz und Selbstähnlichkeit in der Turbulenz, Habilitationsschrift, RWTH Aachen, Shaker Verlag, Aachen.

Oberlack, M., 2001. A unified approach for symmetries in plane parallel turbulent shear flows. J. Fluid Mech. 427, 299–328.

Oberlack, M., 2004. Symmetry methods in turbulent boundary layer theory, IUTAM- Symposium: One Hundred Years of Boundary Layer Research, 12–14 August 2004, DLR- Göttingen.

Pop, I., Ingham, D.B., 2001. Convective Heat Transfer, Mathematical and Computational Modelling of Viscous Fluids and Porous Media, Pergamon, London.

Rees, D.A.S., Magyari, E., Keller, B., 2003. The development of the asymptotic viscous dissipation profile in a vertical free convective boundary layer flow in a porous medium. Transport Porous Media 53, 347–355.